In Vivo Detection of Dendritic Cell Antigen Presentation to $CD4^+$ T Cells

By Elizabeth Ingulli,* Anna Mondino,‡§ Alexander Khoruts,‡§ and Marc K. Jenkins‡§

*From the *Department of Pediatrics, ‡Department of Microbiology, and the §Center for Immunology, University of Minnesota Medical School, Minneapolis, Minnesota 55455*

Summary

Although lymphoid dendritic cells (DC) are thought to play an essential role in T cell activation, the initial physical interaction between antigen-bearing DC and antigen-specific T cells has never been directly observed in vivo under conditions where the specificity of the responding T cells for the relevant antigen could be unambiguously assessed. We used confocal microscopy to track the in vivo location of fluorescent dye-labeled DC and naive TCR transgenic $CD4^+$ T cells specific for an OVA peptide–I-A^d complex after adoptive transfer into syngeneic recipients. DC that were not exposed to the OVA peptide, homed to the paracortical regions of the lymph nodes but did not interact with the OVA peptide-specific T cells. In contrast, the OVA peptide-specific T cells formed large clusters around paracortical DC that were pulsed in vitro with the OVA peptide before injection. Interactions were also observed between paracortical DC of the recipient and OVA peptide-specific T cells after administration of intact OVA. Injection of OVA peptide-pulsed DC caused the specific T cells to produce IL-2 in vivo, proliferate, and differentiate into effector cells capable of causing a delayed-type hypersensitivity reaction. Surprisingly, by 48 h after injection, OVA peptide-pulsed, but not unpulsed DC disappeared from the lymph nodes of mice that contained the transferred TCR transgenic population. These results demonstrate that antigen-bearing DC directly interact with naive antigen-specific T cells within the T cell–rich regions of lymph nodes. This interaction results in T cell activation and disappearance of the DC.

In vitro and in vivo studies have shown that bone marrow–derived dendritic cells (DC)[1] are the most effective APCs at activating naive $CD4^+$ T cells (1). This efficiency is thought to be related to the fact that DC express high levels of class II MHC, adhesion, and costimulatory molecules, which play essential roles in T cell activation (1). In addition, DC are the most abundant class II MHC–expressing APC in the T cell–rich areas of secondary lymphoid tissues, and are thus well-positioned to interact with naive T cells.

Although in vitro experiments strongly indicate that DC are the initiating APC for T cell responses in vivo, suggestive evidence supporting this idea has only recently been reported (2, 3). Proliferating T cells have been observed in contact with the DC of the T cell areas of lymphoid tissue after injection of superantigens (2) or allogeneic cells (3). However, because methodologies did not exist for in situ detection of the few T cells specific for any given peptide–MHC complex in unimmunized individuals, it has not been possible to definitively demonstrate interactions between naive, peptide antigen-specific T cells and antigen-bearing dendritic cells in vivo. To overcome this difficulty, we previously developed (5) an adoptive transfer system in which a small but detectable number of naive DO11.10 TCR transgenic $CD4^+$ cells are injected intravenously into normal syngeneic BALB/c recipients. The majority of the $CD4^+$ T cells in the DO11.10 TCR transgenic mice (6) are specific for a chicken OVA peptide 323-339/I-A^d class II MHC complex (7), and can be detected with the KJ1-26 mAb (8), which is uniquely specific for the DO11.10 clonotypic TCR. We used this system here, to characterize interactions between peptide–MHC-bearing DC and naive antigen-specific $CD4^+$ T cells during in vivo immune responses.

[1]*Abbreviations used in this paper:* CMFDA, 5-chloromethylfluorescein diacetate; CMTMR, 5-(and -6)-(((4-chloromethyl) benzoyl) amino) tetramethylrhodamine; DC, dendritic cell; DTH, delayed-type hypersensitivity; SA, streptavidin.

Materials and Methods

Animals. DO11.10 BALB/c mice were produced by backcrossing the original DO11.10 TCR-transgenic mice (kindly provided by Dr. Dennis Loh) with BALB/c (H-2^d) mice (pur-

 J. Exp. Med. © The Rockefeller University Press • 0022-1007/97/06/2133/09 $2.00
Volume 185, Number 12, June 16, 1997 2133–2141

chased from the National Cancer Institute, Frederick, MD) for >10 generations. DO11.10 BALB/c SCID mice were produced by back-crossing DO11.10 BALB/c mice with BALB/c SCID mice (purchased from the National Cancer Institute, Frederick, MD) for two generations and selecting for offspring that contained DO11.10 T cells and no other lymphocytes (as assessed by flow cytometric analysis of blood cells stained with KJ1-26 and anti-B220 mAbs). All DO11.10 BALB/c and BALB/c SCID mice were bred and housed under specific pathogen-free conditions. 6–8-wk-old, sex-matched mice were used for all experiments. Mice were cared for in accordance with University of Minnesota and NIH guidelines.

Purification and Labeling of CD4$^+$ T Cells. Lymph node cells from DO11.10 or BALB/c donor mice were passed over an anti-CD8 and anti-immunoglobulin column (Biotex, Edmonton, Alberta) to enrich for CD4$^+$ T cells. Lymph node cells from DO11.10 SCID mice were passed over a G10 column to eliminate macrophages. The T cells were labeled with the green fluorescent dye, 5-chloromethylfluorescein diacetate (CMFDA), according to the manufacturer's protocol (Molecular Probes, Eugene, OR) and 2.5×10^6 labeled cells were injected intravenously into syngeneic BALB/c mice.

Isolation and Labeling of DC. Splenic DC were enriched according to the method of Steinman and coworkers (9). In brief, spleen fragments were subjected to mild collagenase digestion at 37°C for 60 min to release DC. Low density cells were selected by centrifugation on a 35% bovine serum albumin gradient (Sigma Chem. Co., St. Louis, MO), cultured in plastic dishes for 1–2 h after which the nonadherent cells were washed away. The adherent cells were cultured overnight with 100 μg/ml of OVA peptide 323-339 (referred to hereafter as OVA peptide) or medium. The DC, which detached from the plates during the incubation period, were collected and labeled with the red fluorescent dye, 5-(and -6)-(((4-chloromethyl) benzoyl) amino) tetramethylrhodamine (CMTMR), according to the manufacturer's protocol (Molecular Probes). DC were injected subcutaneously (0.5×10^6 in 30–50 μl of PBS) into the hind foot pads of recipient mice the day after the DO11.10 T cell transfer. Splenic DC were used instead of the DC that can be obtained from cytokine-stimulated bone marrow cultures, to minimize potential presentation of FCS serum proteins that could lead to background detection of FCS-specific T cells (10).

Flow Cytometry. DC purity was confirmed by flow cytometry as described by Levin et al. (11). In brief, purified DC (10^5) were incubated with FITC-labeled anti-FcR mAb 2.4G2 (PharMingen, San Diego, CA), FITC-labeled anti-B220 mAb RA3-6B2 (PharMingen), biotin-labeled anti-class II MHC mAb M5/114, and PE-labeled streptavidin (SA) (Caltag, South San Francisco, CA) sequentially on ice for 15–20 min, with washes between steps. 10,000 events were collected on a Becton Dickinson FACScan® (Mountain View, CA) flow cytometer and analyzed using Lysis II software. DC were identified as class II MHC$^+$, Fc receptor$^-$, B220$^-$ cells; and ~85% of the cells were DC by these criteria. To obtain the percentage of CD4$^+$, KJ1-26$^+$ cells, popliteal lymph node cells (10^6) were stained with PE-labeled anti-CD4 mAb H129.19 (PharMingen) and biotin-labeled KJ1-26 mAb followed by SA-FITC (Caltag). After washing, 10,000 events were collected and analyzed. For intracellular IL-2 staining, popliteal lymph node cells ($1\text{-}5 \times 10^6$) were stained with CyChrome-labeled anti-CD4 mAb RM4-5 (PharMingen) and biotin-labeled KJ1-26 mAbs followed by SA-FITC. Cells were then fixed in 2% formaldehyde, and permeabilized with 0.5% saponin, as previously described (12, 13). A PE-labeled anti–IL-2 mAb S4B6 (PharMingen) or isotype control mAb R35-95 (PharMingen) was then added to detect cytosolic IL-2. After washing, 1,000–3,000 CD4$^+$, KJ1-26$^+$ or CD4$^+$, KJ1-26$^-$ events were collected and analyzed.

Immunofluorescent Microscopy. Draining popliteal lymph nodes were harvested from sacrificed mice at various times after the DC injections. The lymph nodes were frozen in liquid nitrogen. Cryostat-cut tissue sections (24 μm) were fixed in 4% paraformaldehyde and washed in PBS. In some experiments, lymph node sections (4 μm) were fixed in acetone, blocked with anti-FcR mAb 2.4G2 and stained sequentially with biotin-labeled N418 mAb (anti-CD11c), biotin-labeled goat anti–hamster IgG (Caltag), followed by Cy 3-labeled SA. Confocal microscopy and image analyses were performed as previously described by Brelje et al. (14). In brief, sections were analyzed using a confocal microscope equipped with a krypton/argon laser (MRC-1000; Bio-Rad Life Science Group, Hercules, CA). Separate green and red images were collected for each section analyzed. Final image processing was performed using the Confocal Assistant program (Minneapolis, MN) and Adobe Photoshop (Mountain View, CA). The area (mm^2) of lymph node scanned was measured using MetaMorph software (West Chester, PA). Adjacent tissue sections (4 μm) were stained with biotin-labeled anti-CD4 mAb RM4-5 (PharMingen) and SA-FITC (Caltag) or biotin-labeled anti-B220 mAb RA3-6B2 (PharMingen) and SA-tetramethylrhodamine (Molecular Probes) to identify the paracortical (T cell–rich) and follicular (B cell–rich) regions of the lymph nodes by conventional immunofluorescent microscopy.

Injections. In some experiments, mice were injected subcutaneously in the hind foot pad with a chemical conjugate of OVA and hen egg lysozyme, which was designed for use in T cell/B cell collaboration experiments. This conjugate, and native OVA stimulate DO11.10 T cells identically in vivo (data not shown).

Delayed-type Hypersensitivity Response. 7 d after the initial DC injections, mice were rechallenged with an intradermal injection of soluble OVA (10 μg) in the ears. Ear thickness was measured at the time of injection (baseline) and 24 h later by an individual who was unaware of the experimental design. The degree of response was calculated as the difference between the two measurements.

Results

In Vivo Analysis of Interactions between Antigen-pulsed DC and Antigen-specific CD4$^+$ T Cells. Using immunohistochemical detection with the KJ1-26 mAb, we previously showed that DO11.10 T cells were present in the T cell–rich paracortical regions of all lymph nodes within 24 h of intravenous injection (5). Similarly, intravenously injected, CMFDA-labeled DO11.10 T cells were found in the paracortical regions of the lymph nodes (Fig. 1) 24 h after injection, indicating that the dye labeling process did not affect their trafficking ability. In the absence of antigen, the CMFDA-labeled DO11.10 T cells could be detected via their green fluorescence in the paracortical regions for at least 72 h (data not shown). CMTMR-labeled, unpulsed DC were first detected in the draining lymph nodes 8 h after subcutaneous injection, accumulated to a maximal level by 24 h, and declined slightly by 48 h (Figs. 2 *B* and 3 *A*). By 24 h, the unpulsed DC were found almost exclusively in the paracortical regions of the lymph nodes (Fig. 1 *B*). Despite the paracortical colocalization of the labeled T cells and un-

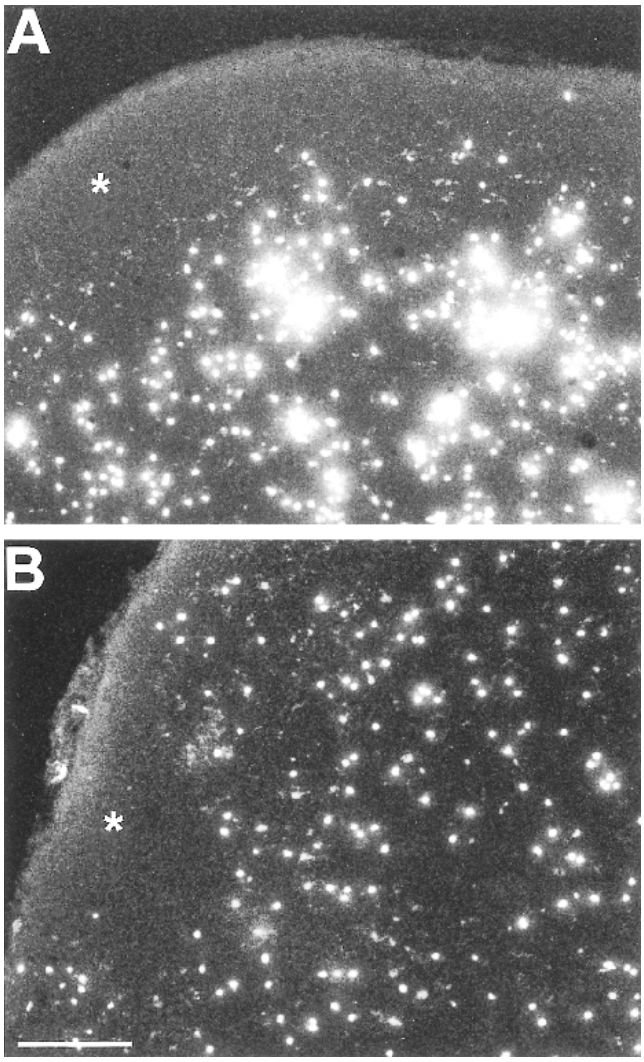

Figure 1. Visualization of OVA peptide–MHC-bearing DC and $CD4^+$ T cell interactions in situ. CMFDA-labeled DO11.10 T cells (*green*) and CMTMR-labeled DC (*red*) were purified, dye-labeled and injected into recipient mice as described in Materials and Methods. Draining popliteal lymph nodes were harvested 24 h after DC injections. Tissue was processed and analyzed by confocal microscopy as described in Materials and Methods. The full-width half peak resolution of the sampling volume was 4.5–5.0 μm; in other words, the optical thickness of each image is 4.5–5 μm. Images were taken from lymph nodes of mice injected with (*A*) OVA peptide-pulsed DC or (*B*) unpulsed DC. Follicular regions, defined on adjacent sections as areas rich in $B220^+$ cells, are indicated (*). Bar, 150 μm.

pulsed DC, few if any interactions between the cells were observed throughout the 48-h observation period (Figs. 1 *B*, 2 *B*, and 3 *B*).

A very different pattern was observed after injection of OVA peptide-pulsed DC. The rate of entry of OVA peptide-pulsed DC into the lymph nodes over the first 24 h was similar to that observed for unpulsed DC (Figs. 2 *A* and 3 *A*). However, at each time point, clusters of DO11.10 T cells (≥2 cells) were observed surrounding the OVA peptide-pulsed DC (Figs. 1 *A*, 2 *A*, and 3 *B*). At 24 h, the time of maximal DC accumulation, ~70% of the OVA peptide-pulsed DC were surrounded by many DO11.10 T cells. In addition, at this magnification, areas of yellow color appeared in the clusters reflecting overlap between the red and green images and close contact between the T cells and DC. The specificity of cluster formation was indicated by the finding that clusters were not observed in mice that received CMFDA-labeled polyclonal BALB/c $CD4^+$ T cells and were injected 24 h previously with CMTMR-labeled OVA peptide-pulsed DC (Fig. 3 *B*).

Although the high degree of coincidence between OVA peptide-pulsed DC and DO11.10 T cell clusters at 24 h made it likely that the clusters represented bona fide interactions between the two cell types, the ~5-μm-thickness of the optical sections made it formally possible that the dendritic cells were not centrally located within the clusters, but rather were situated immediately above or below the clusters. Serial optical sectioning through individual cluster-associated, OVA peptide-pulsed dendritic cells was performed at high power (optical section thickness = 0.6

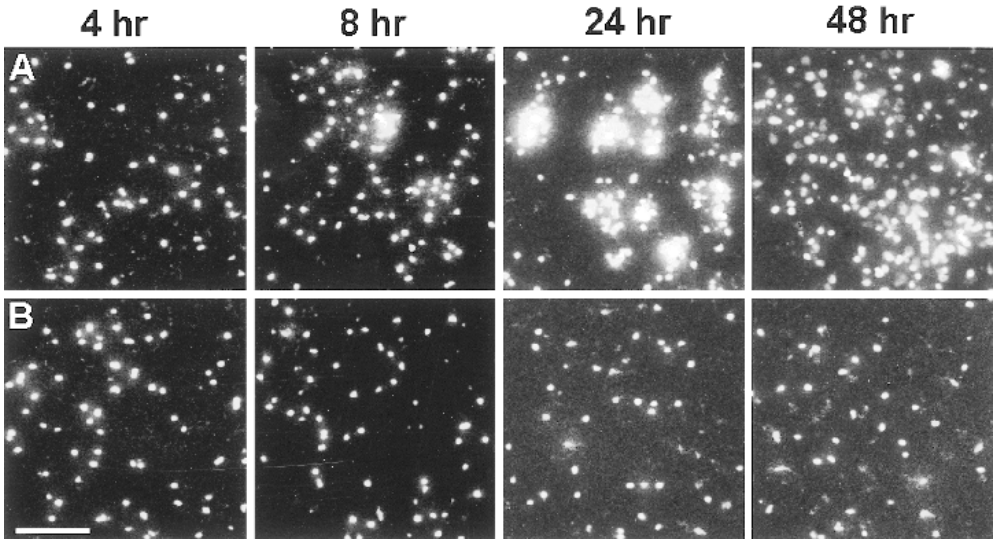

Figure 2. In vivo clustering of OVA peptide–MHC-bearing DC and DO11.10 T cells. DO11.10 T cells (*green*) and DC (*red*) were purified, dye-labeled and injected into recipient mice as described in Materials and Methods. Draining popliteal lymph nodes were harvested 4, 8, 24, and 48 h after DC injections. Tissue was processed and analyzed by confocal microscopy as described in Materials and Methods. The optical thickness of each image is 4.5–5 μm. Images were taken from paracortical regions of lymph nodes of mice injected with (*A*) OVA peptide-pulsed DC or (*B*) unpulsed DC. Bar, 100 μm.

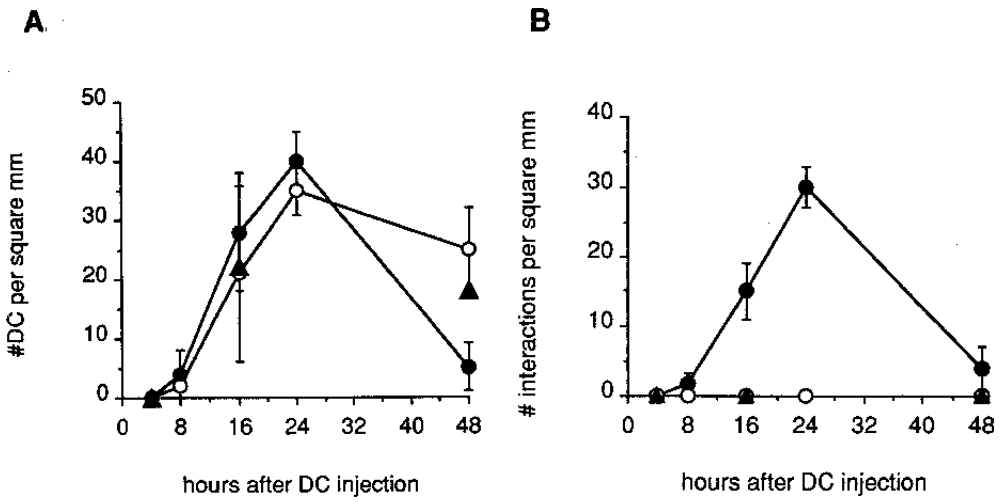

Figure 3. Kinetics of DC appearance and cluster formation in draining lymph nodes. CMFDA-labeled DO11.10 (*circles*) or polyclonal BALB/c (*triangles*) $CD4^+$ T cells were injected intravenously into BALB/c recipient mice the day before CMTMR-labeled OVA peptide-pulsed (*closed symbols*) or unpulsed (*open symbols*) DC were injected subcutaneously into the hind foot pads. Draining popliteal lymph nodes were harvested at the indicated times after DC injection and analyzed with two-color confocal immunofluorescent microscopy as described in Materials and Methods. One image was collected per 24-μm section to ensure that individual fluorescent cells were only counted once. An interaction was defined as two or more green T cells overlapping a red DC such that a yellow area was produced. The number of DC (*A*) and DC engaged in T cell interactions (*B*) were quantified per unit area (mm^2) of lymph node. The results represent the mean values ± SD of 2–3 mice/group (except for the results from the polyclonal BALB/c T cell group, which came from a single animal) derived from a single experiment. Similar values were obtained in two other independent experiments.

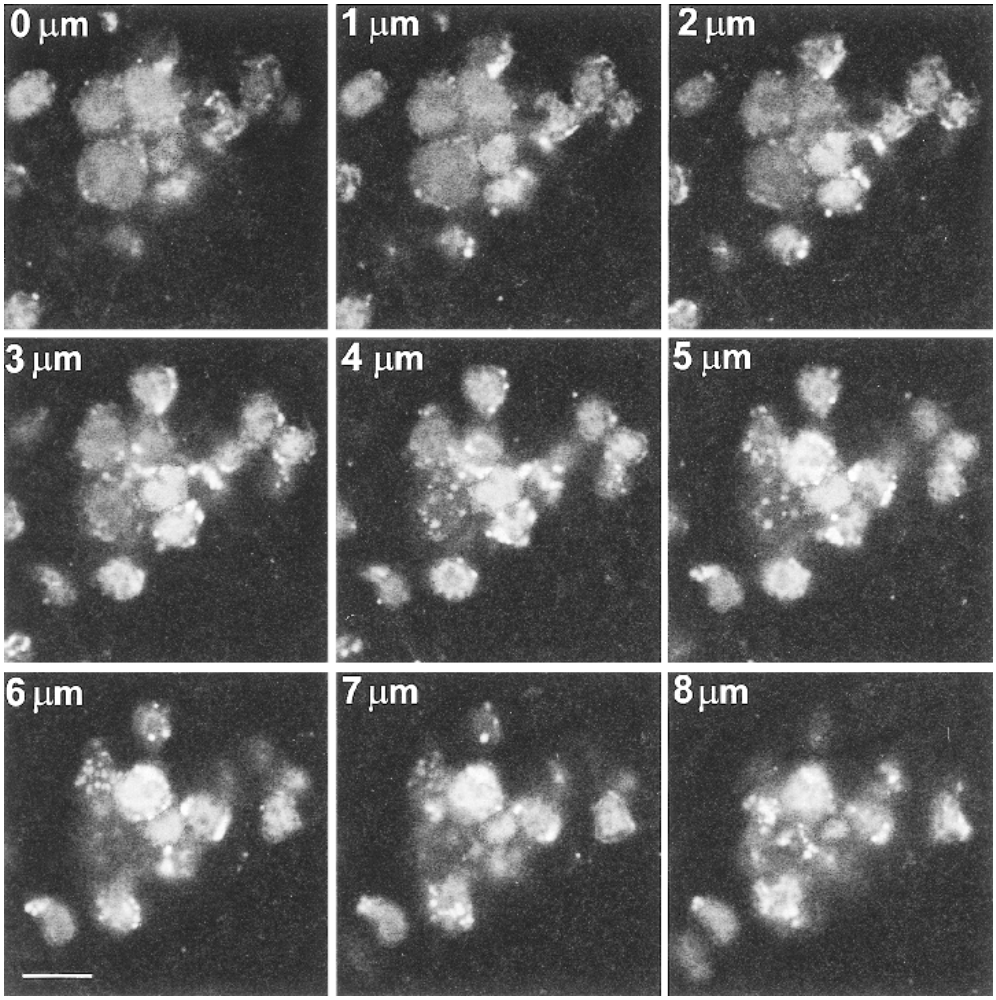

Figure 4. Detailed analysis of a DC–T cell cluster. A series of optical sections was taken at 1-μm intervals through a dendritic cell that appeared to be surrounded by T cells 24 h after the injection of OVA peptide-pulsed DC. At this magnification, the optical thickness of each image is ~0.6 μm. Bar, 10 μm.

μm) to assess this possibility. As shown in Fig. 4, interactions between the dendritic cell and several DO11.10 T cells were observed in each serial plane of focus through the dendritic cell body. Similar results were observed for all clusters examined in this way (n = 5). These results demonstrate that OVA peptide-pulsed dendritic cells are centrally located within the clusters at the 24-h time point, and are simultaneously interacting with many DO11.10 T cells.

48 h after injection, essentially all of the OVA peptide-pulsed DC were surrounded by DO11.10 T cells (Fig. 2 *A*). However, the number of DO11.10 T cells present in the clusters was reduced and the number of OVA peptide-pulsed DC present was lower than was observed in recipients of unpulsed DC at this time (Fig. 3 *A*). The disappearance of OVA peptide-pulsed DC at 48 h appeared to be a function of the presence of DO11.10 T cells and the ability to induce cluster formation, because OVA peptide-pulsed DC persisted to the same degree as unpulsed DC when injected into mice that previously received CMFDA-labeled polyclonal BALB/c T cells (Fig. 3 *A*).

Approximately 75% of the $CD4^+$ cells purified from the DO11.10 mice express the DO11.10 TCR-α and TCR-β chains (6, 15). Because of incomplete allelic exclusion, the remaining 25% express the DO11.10 TCR-β chain with an endogenous TCR-α chain, and are specific for antigens other than OVA (15). DO11.10 mice were backcrossed with SCID mice, which produce endogenous TCR-α chains only at very low levels, to exclude the possibility that endogenous TCR-α chain–expressing T cells were interacting with the DC. Flow cytometric analysis of lymph node cells from DO11.10 SCID mice confirmed that essentially all of the $CD4^+$ T cells in these mice also stained with the KJ1-26 mAb (data not shown). CMFDA-labeled DO11.10 SCID T cells clustered around 36 ± 3% of the CMTMR-labeled, OVA peptide-pulsed DC and 0 ± 0% of the CMTMR-labeled unpulsed DC, 24 h after DC injection.

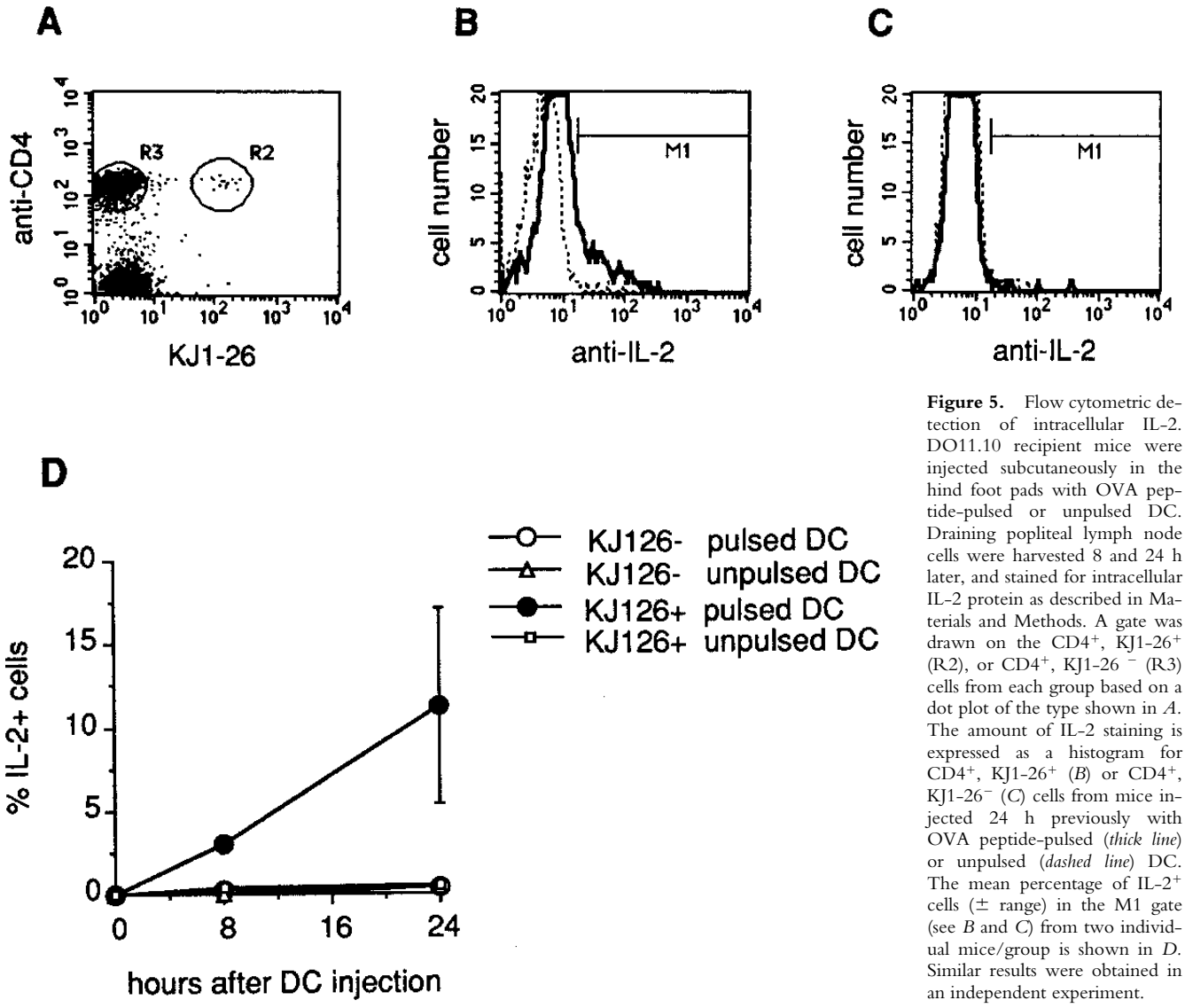

Figure 5. Flow cytometric detection of intracellular IL-2. DO11.10 recipient mice were injected subcutaneously in the hind foot pads with OVA peptide-pulsed or unpulsed DC. Draining popliteal lymph node cells were harvested 8 and 24 h later, and stained for intracellular IL-2 protein as described in Materials and Methods. A gate was drawn on the $CD4^+$, KJ1-26^+ (R2), or $CD4^+$, KJ1-26^- (R3) cells from each group based on a dot plot of the type shown in *A*. The amount of IL-2 staining is expressed as a histogram for $CD4^+$, KJ1-26^+ (*B*) or $CD4^+$, KJ1-26^- (*C*) cells from mice injected 24 h previously with OVA peptide-pulsed (*thick line*) or unpulsed (*dashed line*) DC. The mean percentage of IL-2^+ cells (± range) in the M1 gate (see *B* and *C*) from two individual mice/group is shown in *D*. Similar results were obtained in an independent experiment.

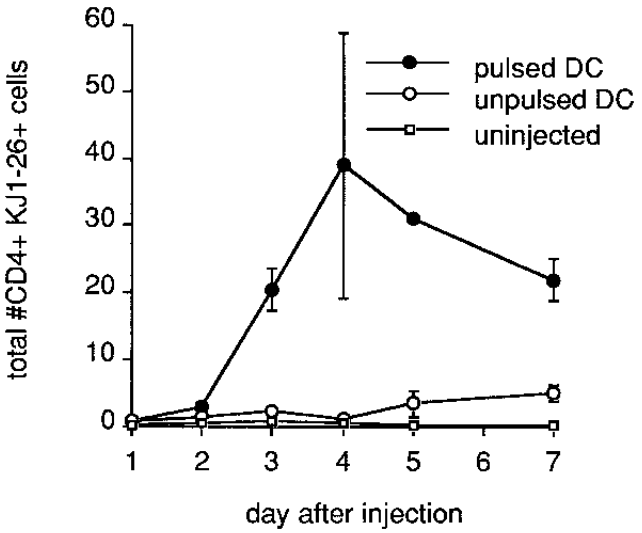

Figure 6. Kinetics of clonal expansion induced by injection of OVA peptide-pulsed or unpulsed DC. BALB/c recipients of DO11.10 T cells were injected subcutaneously in the hind foot pad with 0.5×10^6 OVA peptide-pulsed DC (*closed circles*), 0.5×10^6 unpulsed DC (*open circles*), or nothing (*open squares*). The draining popliteal lymph nodes were harvested at various time points after injection. Flow cytometric analysis was performed on 10,000 lymph node cells from each group after staining to obtain the percentage of $CD4^+$, KJ1-26^+ cells present at each time point. The total number of $CD4^+$, KJ1-26^+ cells was calculated by multiplying the percentage of $CD4^+$, KJ1-26^+ cells by the total number of lymph node cells obtained from a viable cell count. The results represent the mean values ± range of two mice from a single experiment. Similar values were obtained from three other independent experiments.

In this same experiment, we found that CMFDA-labeled DO11.10 SCID T cells also failed (0 ± 0%) to cluster around CMTMR-labeled unpulsed DC in mice that also received unlabeled OVA peptide-pulsed DC at the same time. Together these results demonstrated that $CD4^+$ T cells expressing the DO11.10 TCR were responsible for cluster formation and that cluster formation required that the OVA peptide-pulsed DC present the relevant peptide–MHC complex. Furthermore, because the DO11.10 SCID T cells uniformly expressed a naive surface phenotype ($CD45RB^{high}$, L-$selectin^{high}$) at the time of adoptive transfer (15, data not shown), these results also demonstrate that naive antigen-specific T cells interact with peptide–MHC-bearing DC in vivo.

The physical interactions between the DO11.10 T cells and OVA peptide-pulsed DC correlated with activation of the T cells. Intracellular staining with anti–IL-2 antibody showed that a significant fraction of the DO11.10 T cells present in recipients injected with OVA peptide-pulsed DC at the time of maximal cluster formation (24 h) were producing the growth factor IL-2 (Fig. 5, *B* and *D*). The specificity of this response was demonstrated by the finding that IL-2 production was not detected in DO11.10 cells from mice injected with unpulsed DC (Fig. 5, *B* and *D*) or in the $CD4^+$, KJ1-26^- T cells (recipient T cells) present in mice injected with OVA peptide-pulsed DC (Fig. 5, *C* and *D*).

48 h after injection of OVA peptide-pulsed DC about one-third of the CMFDA-labeled DO11.10 T cells were dull green (Fig. 2 *A*), perhaps because of dilution of the dye as a consequence of cell division. By 72 h, the number of DO11.10 T cells in mice injected with OVA peptide-pulsed DC, but not unpulsed DC increased dramatically in the draining lymph nodes, and this increase continued to a peak at 96 h (Fig. 6). Normal mice or recipients of DO11.10 T cells that had been injected with DC 7 d earlier were rechallenged with soluble OVA subcutaneously in the ear to determine if T cells capable of causing an OVA-specific DTH response had been induced. DO11.10 recipient mice that had been previously injected with OVA peptide-pulsed DC, but not unpulsed DC mounted a strong DTH reaction that surpassed that of similarly primed BALB/c mice that did not receive DO11.10 T cells (Fig. 7), suggesting that the DO11.10 T cells participated in the delayed-type hypersensitivity (DTH) reaction in the former situation.

In Vivo Analysis of Interactions Between Resident Lymph Node DC and Antigen-specific $CD4^+$ T Cells after Injection of Soluble Antigen. Finally, we determined whether the unlabeled endogenous DC of the recipient could form clusters with CMFDA-labeled DO11.10 T cells in vivo after injection of a soluble form of intact OVA to ensure that cluster formation was a property of DC that had not been through the purification and labeling process. As shown in Fig. 8, in the absence of OVA, CMFDA-labeled DO11.10 SCID T cells were not clustered and were rarely found interacting with endogenous paracortical DC (Fig. 8 *B*). In contrast, 24 h after injection of OVA, CMFDA-labeled DO11.10 T cells formed small clusters, many of which showed evidence (*yellow*) of interactions with endogenous paracortical DC of the recipient (Fig. 8 *A*).

Discussion

The ability to physically monitor the anatomic location of naive antigen-specific T cells and DC allowed us to reach several conclusions about antigen presentation in vivo. Because T cell/DC clusters were only observed when a high frequency of OVA peptide-specific T cells and OVA peptide–MHC-bearing DC were present at the same time is strong evidence that the clusters represent antigen presentation events. This conclusion is further supported by the findings that cluster formation coincided with IL-2 production by the antigen-specific T cells, and was followed by proliferation and differentiation of the T cells into DTH effector cells. Our results are consistent with those of others who showed that clusters of proliferating T cells are found in proximity to T cell zone DC after injection of superantigens (2) or allogeneic cells (3). The capacity of individual OVA peptide-pulsed DC to simultaneously interact with many antigen-specific T cells in vivo is reminiscent of the in vitro studies of Steinman and coworkers (16–19), and provides a possible explanation for the ability of small numbers of tumor peptide-pulsed DC to induce cancer im-

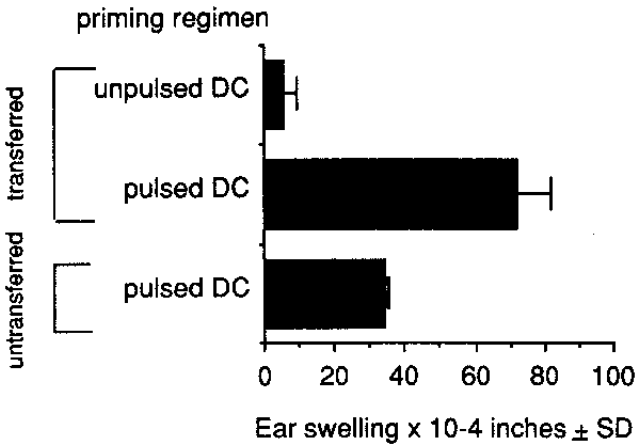

Figure 7. DTH response. DO11.10 recipient mice were injected subcutaneously in the hind foot pad with 0.5×10^6 OVA peptide-pulsed or unpulsed DC. In addition, normal BALB/c mice were injected with 0.5×10^6 OVA peptide-pulsed DC. 7 d after the initial injection, all mice were rechallenged with an intradermal injection of soluble intact OVA (10 μg) in the ears. The results represent the mean ear swelling values ± SD of 2–4 ears/group derived from a single experiment. Similar values were obtained from three other independent experiments.

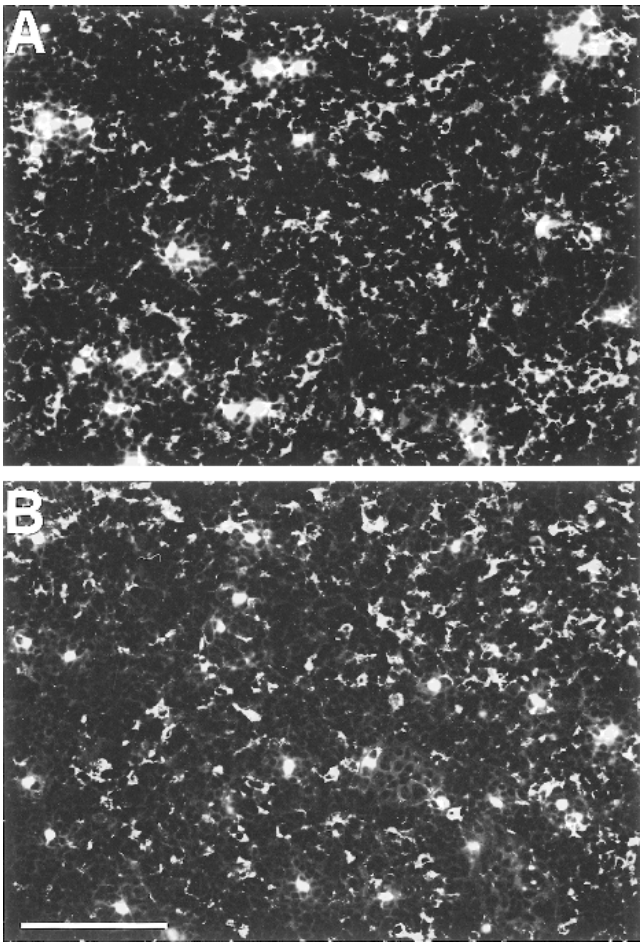

Figure 8. Endogenous DC cluster DO11.10 T cells in the presence of antigen. DO11.10 SCID T cells were purified, CMFDA-labeled (*green*), and injected into recipient mice as described in Materials and Methods. The next day recipient mice were injected subcutaneously with 45 μg of OVA–hen egg lysozyme conjugate (*A*) or nothing (*B*). 24 h later, draining popliteal lymph nodes were harvested, sectioned, fixed in acetone, and stained sequentially with biotin-labeled DC-specific mAb N418, biotin-labeled goat anti–hamster IgG and Cy 3–labeled SA to detect endogenous paracortical DC (*red*). Tissue was analyzed by confocal microscopy as described in Materials and Methods. The optical thickness of each image is 2–3 μm. Images shown were from paracortical regions of the lymph nodes. Bar, 100 μm.

munity (20, 21). It should also be noted that DO11.10 T cells formed clusters around endogenous DC following soluble OVA injection indicating that indeed DC play an important role in antigen presentation in vivo. In this situation, however, DC–T cell clusters are smaller probably because all of the DC have access to antigen and are thus in competition with each other for antigen presentation to the DO11.10 T cells.

The finding that very few DO11.10 T cells were found in proximity to unpulsed DC despite colocalization to the lymph node paracortex indicates that interactions between antigen-specific $CD4^+$ T cells and DC in the absence of the relevant antigen are very transient. It is possible that these transient interactions are stabilized if the DC display the appropriate peptide–MHC complexes and activate the interacting T cells to upregulate the activity of their adhesion molecules (22). The subsequent stable binding between antigen-specific T cells and antigen-presenting DC would allow sustained TCR signaling, which has been shown to be required for T cell commitment to lymphokine production (23). An alternative possibility is that naive T cells are first activated by an APC from the recipient before binding to the OVA peptide-pulsed, labeled DC. This is unlikely because it would require transfer of OVA peptide from the labeled DC to recipient APCs. This does not appear to be the case because injection of OVA peptide-pulsed, unlabeled DC together with unpulsed, labeled DC into recipients containing labeled DO11.10 T cells did not result in cluster formation between the labeled populations as would be expected if peptide transfer occurred.

It was surprising to find that OVA peptide-pulsed, CMTMR-labeled DC rapidly disappeared from the lymph nodes after the time of maximal interaction with DO11.10 T cells. It is possible that activation caused the labeled DC to metabolize the dye and become undetectable. CD40 signaling has been shown to stimulate cytokine production and costimulatory molecule expression in DC, and the activated DO11.10 T cells present in the clusters would be expected to express CD40 ligand (24). However, if dye metabolism due to DC activation was the only explanation, then many DO11.10 T cell clusters lacking a labeled DC should have been observed. This was not the case; many fewer clusters were present at 48 h but most contained a labeled DC. Thus, a more likely explanation is that the DC physically disappear because they migrate out of the lymph node or are killed by the responding T cells. $CD4^+$ T cell killing of the cognate APC has been described in several cases (25, 26). In addition, a recent study by De Smedt et al.

(27) showed that LPS also induces the activation and then disappearance of DC in the spleen. Therefore, DC activation by inflammatory cytokines or cognate interactions with antigen-specific T cells may eventually lead to elimination of the DC, allowing any interacting T cells to disengage. By escaping from antigen-presenting DC, activated T cells would be free to proliferate, interact with other APCs such as antigen-specific B cells within the follicles, and eventually to migrate out of the lymph node to non-lymphoid sites of inflammation. Transient elimination of antigen-presenting DC would also provide a mechanism for terminating T cell responses, that could do damage if allowed to go on unchecked.

The authors thank Drs. M. Mescher, D. Mueller, and S. Jameson for critically reading the manuscript; R. Merica, K.A. Pape and Z.M. Chen for helpful discussions; and J. White for technical assistance.

This work was supported by National Institutes of Health grants AI27998, AI35296, AI39614 (M.K. Jenkins), DK07087 (E. Ingulli), the Vikings Children's Fund (E. Ingulli), the Howard Hughes Medical Institute (A. Khoruts), and Glaxo Wellcome (A. Khoruts).

Address correspondence to Elizabeth Ingulli, Department of Pediatrics, University of Minnesota Medical School, Box 491 UMHC, 420 Delaware St. S.E., Minneapolis, MN 55455.

Received for publication 28 February 1997 and in revised form 16 April 1997.

References

1. Steinman, R.M. 1991. The dendritic cell system and its role in immunogenicity. *Annu. Rev. Immunol.* 9:271–296.
2. Luther, S.A., A. Gulbranson-Judge, H. Acha-Orbea, and I. MacLennan. 1997. Viral superantigen drives extrafollicular and follicular B cell differentiation leading to virus-specific antibody production. *J. Exp. Med.* 185:551–562.
3. Kudo S., K. Matsuno, T. Ezaki, and M. Ogawa. 1997. A novel migration pathway for rat dendritic cells from the blood: hepatic sinusoids-lymph translocation. *J. Exp. Med.* 185:777–784.
4. Tse, H.Y., R.H. Schwartz, and W.E. Paul. 1980. Cell-cell interactions in the T cell proliferative response. *J. Immunol.* 125:401–500.
5. Kearney, E.R., K.A. Pape, D.Y. Loh, and M.K. Jenkins. 1994. Visualization of peptide-specific T cell immunity and peripheral tolerance induction in vivo. *Immunity.* 1:327–339.
6. Murphy, K.M., A.B. Heimberger, and D.Y. Loh. 1990. Induction by antigen of intrathymic apoptosis of $CD4^+CD8^+$ TCR^{lo} thymocytes in vivo. *Science (Wash. DC).* 250:1720–1723.
7. Shimonkevitz, R., S. Colon, J.W. Kappler, P. Marrack, and H.M. Grey. 1984. Antigen recognition by H-2-restricted T cells. II. A tryptic ovalbumin peptide that substitutes for processed antigen. *J. Immunol.* 133:2067–2074.
8. Haskins, K., R. Kubo, J. White, M. Pigeon, J. Kappler, and P. Marrack. 1983. The MHC-restricted antigen receptor on T cells. I. Isolation of a monoclonal antibody. *J. Exp. Med.* 157:1149–1169.
9. Swiggard, W.J., R.M. Nonacs, M.D. Witmer-Pack, R.M. Steinman, and K. Inaba. 1991. Enrichment of dendritic cells by plastic adherence and EA rosetting. *In* Current Protocols in Immunology. J.E. Coligan, A.M. Kruisbeek, D.H. Margulies, E.M. Shevach, and W. Strober, editors. John Wiley and Sons, New York. 3.7.1–3.7.11.
10. Inaba, K., M. Inaba, N. Romani, H. Aya, M. Deguchi, S. Ikehara, S. Maramatsu, and R.M. Steinman. 1992. Generation of large numbers of dendritic cells from mouse bone marrow cultures supplemented with granulocyte/macrophage colony-stimulating factor. *J. Exp. Med.* 176:1693–1702.
11. Levin, D., S. Constant, T. Pasqualini, R. Flavell, and K. Bottomly. 1993. Role of dendritic cells in the priming of $CD4^+$ T lymphocytes to peptide antigen in vivo. *J. Immunol.* 151: 6742–6750.
12. Assenmacher, M., J. Schmitz, and A. Radbruch. 1994. Flow cytometric determination of cytokines in activated murine T helper lymphocytes: expression of interleukin-10 in interferon-γ and interleukin-4-expressing cells. *Eur. J. Immunol.* 24:1097–1101.
13. Openshaw P., E.E. Murphy, N.A. Hosken, V. Maino, K. Davis, K. Murphy, and A. O'Garra. 1995. Heterogeneity of intracellular cytokine synthesis at the single-cell level in polarized T helper 1 and T helper 2 populations. *J. Exp. Med.* 182:1357–1367.
14. Brelje T.C., M.W. Wessendorf, and R.L. Sorenson. 1993. Multi-color laser scanning confocal immunofluorescence microscopy: practical application and limitations. *Methods Cell Biol.* 38:97–181.
15. Lee, W.T., J. Cole-Calkins, and N.E. Street. 1996. Memory T cell development in the absence of specific antigen priming. *J. Immunol.* 157:5300–5307.
16. Flechner, E.R., P.S. Freudenthal, G. Kaplan, and R.M. Steinman. 1988. Antigen-specific T lymphocytes efficiently cluster with dendritic cells in the human primary mixed-leukocyte reaction. *Cell. Immunol.* 111:183–195.
17. Inaba, K., M. Witmer, and R.M. Steinman. 1984. Clustering of dendritic cells, helper T lymphocytes, and histocompatible B cells during primary antibody responses in vitro. *J. Exp. Med.* 160:858–876.
18. Inaba, K., and R.M. Steinman. 1986. Accessory cell–T lymphocyte interactions. *J. Exp. Med.* 163:247–261.
19. Austyn, J.M., D.E. Weinstein, and R.M. Steinman. 1988. Clustering with dendritic cells precedes and is essential for T-cell proliferation in a mitogenesis model. *Immunology.* 63:691–696.
20. Mayordomo J.I., T. Zorina, W.J. Storkus, L. Zitvogel, C. Celluzzi, L.D. Falo, C.J. Melief, S.T. Illstad, W.M. Kast, A.B. Deleo, and M.T. Lotze. 1995. Bone marrow-derived dendritic cells pulsed with synthetic tumour peptides elicit protective and therapeutic antitumor immunity. *Nat. Med.* 1:

1297–1302.
21. Steinman, R.M. 1996. Dendritic cells and immune-based therapies. *Exp. Hematology*. 24:859–862.
22. Dustin, M.L., and T.A. Springer. 1989. T cell receptor cross-linking transiently stimulates adhesiveness through LFA-1. *Nature (Lond.)*. 341:619–624.
23. Valitutti S., M. Dessing, K. Aktories, H. Gallati, and A. Lanzavecchia. 1995. Sustained signaling leading to T cell activation results from prolonged T cell receptor occupancy. Role of T cell actin cytoskeleton. *J. Exp. Med.* 181:577–584.
24. Noelle, R.J. 1996. CD40 and its ligand in host defense. *Immunity*. 4:415–419.
25. Tite, J.P. 1990. Evidence of a role for TNF-alpha in cytolysis by $CD4^+$, class II MHC-restricted cytotoxic T cells. *Immunology*. 71:208–212.
26. Rathmell, J.C., M.P. Cooke, W.Y. Ho, J. Grein, S.E. Townsend, M.M. Davis, and C.C. Goodnow. 1995. CD95 (Fas)-dependent elimination of self-reactive B cells upon interaction with $CD4^+$ T cells. *Nature (Lond.)*. 376:181–184.
27. De Smedt, T., B. Pajak, E. Muraille, L. Lespagnard, E. Heinen, P. De Baetselier, J. Urbain, O. Leo, and M. Moser. 1996. Regulation of dendritic cell numbers and maturation by lipopolysaccharide in vivo. *J. Exp. Med*. 184:1413–1424.